

Extreme value statistics and arcsine laws for heterogeneous diffusion processes

Prashant Singh *

International Centre for Theoretical Sciences, Tata Institute of Fundamental Research, Bengaluru 560089, India



(Received 22 December 2021; accepted 26 January 2022; published 9 February 2022)

Heterogeneous diffusion with a spatially changing diffusion coefficient arises in many experimental systems such as protein dynamics in the cell cytoplasm, mobility of cajal bodies, and confined hard-sphere fluids. Here, we showcase a simple model of heterogeneous diffusion where the diffusion coefficient $D(x)$ varies in a power-law way, i.e., $D(x) \sim |x|^{-\alpha}$ with the exponent $\alpha > -1$. This model is known to exhibit anomalous scaling of the mean-squared displacement (MSD) of the form $\sim t^{\frac{2}{2+\alpha}}$ and weak ergodicity breaking in the sense that ensemble averaged and time averaged MSDs do not converge. In this paper, we look at the extreme value statistics of this model and derive, for all α , the exact probability distributions of the maximum spatial displacement $M(t)$ and arg-maximum $t_m(t)$ (i.e., the time at which this maximum is reached) till duration t . In the second part of our paper, we analyze the statistical properties of the residence time $t_r(t)$ and the last-passage time $t_\ell(t)$ and compute their distributions exactly for all values of α . Our study unravels that the heterogeneous version ($\alpha \neq 0$) displays many rich and contrasting features compared to that of the standard Brownian motion (BM). For example, while for BM ($\alpha = 0$), the distributions of $t_m(t)$, $t_r(t)$, and $t_\ell(t)$ are all identical (à la “arcsine laws” due to Lévy), they turn out to be significantly different for nonzero α . Another interesting property of $t_r(t)$ is the existence of a critical α (which we denote by $\alpha_c = -0.3182$) such that the distribution exhibits a local maximum at $t_r = t/2$ for $\alpha < \alpha_c$ whereas it has minima at $t_r = t/2$ for $\alpha \geq \alpha_c$. The underlying reasoning for this difference hints at the very contrasting natures of the process for $\alpha \geq \alpha_c$ and $\alpha < \alpha_c$ which we thoroughly examine in our paper. All our analytical results are backed by extensive numerical simulations.

DOI: [10.1103/PhysRevE.105.024113](https://doi.org/10.1103/PhysRevE.105.024113)

I. INTRODUCTION

Many real-world systems involve the motion of tracer particles in a heterogeneous medium with substantial spatial variations of the diffusion coefficient. For example, in [1,2], the dynamics of protein in the cell cytoplasm was shown to exhibit a systematic spatial variation of the diffusion coefficient by using mesoscopic numerical methods. Similarly, the mobility of cajal bodies (nuclear organelles) inside living cells develops heterogeneity due to their interactions with other nuclear components [3]. Other examples of heterogeneous diffusion include particles moving between nearly parallel plates [4], diffusion in the presence of a temperature gradient [5], diffusion in nanoporous solids [6], confined hard-sphere fluids [7], and so on. Descriptions with a space-dependent diffusion coefficient have also been useful in modeling the diffusion in turbulent media [8] and on fractal objects [9]. Quite recently, several studies on heterogeneous diffusive processes (HDPs) have revealed anomalous scaling of the mean-squared displacement (MSD) and weak ergodicity breaking between time averaged and ensemble averaged MSDs [10–16]. Persistent properties of HDPs have also been investigated in [17]. Extensions of HDPs driven by colored noises were considered in [18–20]. Rigorous efforts have also been made to understand the combined effect of HDPs and other models such as

fractional Brownian motion [21] and scaled Brownian motion [22].

In this paper, we analyze a simple model of one-dimensional HDPs where the diffusion coefficient has a power-law dependence on the position of the particle, i.e., $D(x) \sim |x|^{-\alpha}$ with $\alpha > -1$. For $\alpha = 0$, it reduces to the homogeneous case of standard Brownian motion (BM). While the BM is extensively studied in the literature and a large number of results are known, the amount of studies for HDPs is still far from exhaustive. In an attempt toward this direction, we here investigate the extreme value statistics (EVS) of the HDP with power-law form for $D(x)$. In particular, we study how heterogeneity ramifies the statistics of the maximum $M(t)$ of the trajectory $x(t)$ observed till time t and the time $t_m(t)$ at which this maximum is achieved. A schematic illustration of $M(t)$ and $t_m(t)$ for a trajectory is shown in Fig. 1.

For one-dimensional BM ($\alpha = 0$), the marginal distributions of $M(t)$ and $t_m(t)$ read [23]

$$P_m(M|t) = \frac{1}{\sqrt{\pi D_0 t}} \exp\left(-\frac{M^2}{4D_0 t}\right), \quad (1)$$

$$\mathcal{P}_m(t_m|t) = \frac{1}{\pi \sqrt{t_m(t-t_m)}}, \quad (2)$$

where D_0 is the diffusion coefficient. Beyond BM, such studies have also been performed for other stochastic processes such as constrained Brownian motion, random walks and their generalizations [23–31], random acceleration [32–34], active

*prashant.singh@icts.res.in

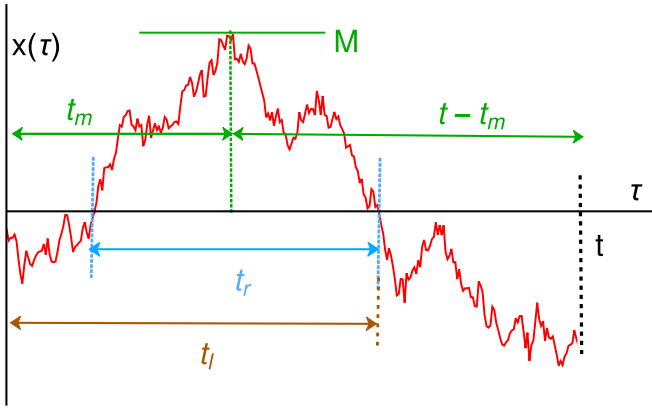


FIG. 1. A schematic illustration of the maximum distance M attained by the process $x(\tau)$ (shown in red) in Eq. (5) till duration t , i.e., $M(t) = \max\{x(\tau)\}$, where $0 \leq \tau \leq t$. The time t_m represents the time at which this maximum is attained. The time t_r represents the amount of time for which $x(\tau)$ stays in the positive semiaxis and the duration t_ℓ is the last time that the process changes its sign (or crosses the origin).

particles [35,36], fractional Brownian motion [37–39], continuous time random walks [40], random matrices [41–43], fluctuating interfaces [44–46], transport models [47–49], finance [50], and other physical systems [51–55] (see [56–65] for review). The subject of extreme value statistics has found applications in ecology [66], computer science [67–69], and convex hull problems [70]. Generalizing these studies, the statistics of the time between maximum and minimum spatial displacements was also recently considered for Brownian motion and random walks in [71,72].

Even though there has been a substantial amount of study on EVS, most of these studies, are based on a homogeneous setup. On the other hand, we saw above that, in many physical situations, the heterogeneous description becomes more relevant. A natural question then is, what happens to the distributions of $M(t)$ and $t_m(t)$ in Eqs. (1) and (2) when the dynamics takes place in a heterogeneous medium? Our work aims to provide a systematic understanding to this question in the context of HDPs with a power-law form of $D(x)$. Our study demonstrates that the extremal statistics of this model is rather rich and possesses many contrasting features compared to that of the BM.

In the second part of our paper, we investigate the properties of the following two quantities measured along a trajectory $x(t)$ observed till time t : (i) residence time $t_r(t)$ spent on the positive (or negative) semiaxis and (ii) the last time $t_\ell(t)$ that the particle crosses the origin. For a trajectory of the particle, these two quantities are illustrated in Fig. 1. The celebrated *arcsine laws* for one-dimensional Brownian motion state that the probability distributions of $t_m(t)$, $t_r(t)$, and $t_\ell(t)$ are all exactly the same and given by [23,73]

$$\mathcal{P}_i(t_i|t) = \frac{1}{\pi \sqrt{t_i(t - t_i)}}, \quad (3)$$

where $t_i \in \{t_m, t_r, t_\ell\}$. The corresponding cumulative probability has the “arcsine” form

$$\text{Prob}[t_i \leq t] = \frac{2}{\pi} \arcsine\left(\sqrt{\frac{t_i}{t}}\right), \quad (4)$$

and hence the name *arcsine laws*. Over the years, these quantities have been studied in different contexts such as Brownian motion, random walks and their generalizations [73–80], random acceleration [32,81], continuous time random walks [40,82], fractional Brownian motion [38], run-and-tumble particles [35,83], finance [50,84,85], renewal processes, and other processes [86–90]. Quite recently, arcsine laws have also been studied both experimentally and theoretically in stochastic thermodynamics [91,92]. The statistics of residence time has also been used to classify the nonergodicity in continuous-time random walk models [93,94]. Here, we look at the statistics of $t_r(t)$ and $t_\ell(t)$ in conjunction with $t_m(t)$ for the HDPs with a power-law form of $D(x)$. More specifically, our interest is to study the ramifications of heterogeneity on the distributions of these three observables. We find that while their distributions are exactly the same for $\alpha = 0$ (BM), they turn out to be significantly different for nonzero α . Our work provides the exact expression of the probability distributions of $M(t)$, $t_m(t)$, $t_r(t)$, and $t_\ell(t)$ for all $\alpha > -1$.

The remainder of paper is structured as follows: We define our model in Sec. II and also present all our main results here. Section III presents the derivation of the joint distribution of $M(t)$ and $t_m(t)$ which is then used to obtain the marginal distribution of $M(t)$ in Sec. III C and that of $t_m(t)$ in Sec. III D. We next compute the distributions of residence time $t_r(t)$ and last-passage time $t_\ell(t)$ in Secs. IV and V, respectively. Finally, we conclude in Sec. VI.

II. MODEL AND SUMMARY OF RESULTS

We study the motion of a particle in one dimension moving in a heterogeneous medium. The heterogeneity is administered by considering the position-dependent diffusion coefficient $D(x)$. The time evolution equation for the position of the particle reads

$$\frac{dx}{dt} = \sqrt{2D(x)}\eta(t), \quad (5)$$

where $\eta(t)$ is the Gaussian white noise with zero mean and correlation $\langle \eta(t)\eta(t') \rangle = \delta(t - t')$. In this paper, we focus on the power-law form of the diffusion coefficient:

$$D(x) = \frac{D_0 l^\alpha}{|x|^\alpha}, \quad \text{with } \alpha > -1, \quad (6)$$

where D_0 is a positive constant that sets the strength of the noise and l is the length scale over which $D(x)$ changes. The exponent α quantifies the strength of the gradient of $D(x)$. Throughout this paper, we consider $\alpha > -1$ and choose the starting position at the origin (unless specified). Note that for $\alpha = 0$, $D(x) = D_0$ is just a constant and we recover the standard Brownian motion (BM). However, our main interest, in this paper, lies in $\alpha \neq 0$ and comparing it with the BM.

Recall that the Langevin equation (5) does not uniquely specify the model for the position-dependent diffusion coefficient and one also needs to specify the sense in which

the stochastic integration of Eq. (5) is carried out [95,96]. Throughout this paper, we will interpret Eq. (5) in the Ito sense. Another problem that one encounters in simulation is that $D(x)$ diverges as $|x| \rightarrow 0$ for $\alpha > 0$ while it tends to zero for $\alpha < 0$. This will cause the shooting off of particles to the infinity for $\alpha > 0$ or accumulation around $x = 0$ for $\alpha < 0$. In order to avoid this problem in simulation, we deploy the following form of $D(x)$ in simulation:

$$D(x) = \lim_{x_{\text{off}} \rightarrow 0^+} \frac{D_0 t^\alpha}{(|x| + x_{\text{off}})^\alpha} \quad (\text{for simulation}). \quad (7)$$

On the other hand, for all our analytic calculations, we take the form of $D(x)$ in Eq. (6). Such x_{off} considerations of $D(x)$ with power-law form have also been studied in [10–12]. For general α , the mean-squared displacement of $x(t)$ in Eq. (5) scales with time as $\langle x^2(t) \rangle \sim t^{\frac{2}{2+\alpha}}$ implying subdiffusive behavior for $\alpha > 0$, superdiffusive for $\alpha < 0$, and diffusive for $\alpha = 0$ [11]. Recently, this model was shown to display weak ergodicity breaking in the sense that time averaged and ensemble averaged MSDs are not identical [10].

Here, we look at the statistical properties of the maximum value $M(t)$ that the position $x(t)$ of the particle attains till duration t , i.e., $M(t) = \max\{x(\tau)\}$, where $0 \leq \tau \leq t$ (see Fig. 1). In conjunction to this, we also investigate the statistics of the time $t_m(t)$ at which this maximum is reached. Exploiting the path-decomposition method for Markov processes [24], we derive exact expression for the joint distribution of $M(t)$ and $t_m(t)$ for all values of α . Marginalizing this joint distribution provides the exact form of the distributions of $M(t)$ and $t_m(t)$.

Next, we also look at the statistics of residence time $t_r(t)$ which refers to the amount of time that the particle stays in the $x > 0$ region till duration t . Formally, it is written as $t_r(t) = \int_0^t d\tau \Theta(x(\tau))$, where $\Theta(x)$ denotes the Heaviside theta function. Using the Feynman-Kac formalism [73,97], we compute the exact probability distribution of $t_r(t)$ for all values of α . Finally, we study the last time $t_\ell(t)$ that the process $x(\tau)$ in Eq. (5) changes sign (or crosses the origin) till duration t and derive exact probability distribution for $t_\ell(t)$. A schematic illustration of M, t_m, t_r , and t_ℓ for a typical trajectory of the particle is shown in Fig. 1. Here, we summarize our main results:

(1) For general α , we derive the exact probability distribution of the maximum M . Denoting this distribution by $P_m(M|t)$, we show that it possesses a scaling behavior of the form

$$P_m(M|t) = \frac{1}{(D_\alpha t)^{\frac{1}{2+\alpha}}} \mathcal{F}_\alpha \left(\frac{M}{(D_\alpha t)^{\frac{1}{2+\alpha}}} \right), \quad (8)$$

where D_α is a constant given in Eq. (24) and the scaling function $\mathcal{F}_\alpha(z)$ is defined as

$$\mathcal{F}_\alpha(z) = \frac{\mathcal{H}_{\frac{1}{2+\alpha}}(0)}{z^{3+\alpha}} \int_0^\infty dw e^{-\frac{w}{z^{2+\alpha}}} \mathbb{H}_{\frac{1}{2+\alpha}}(\sqrt{w}), \quad (9)$$

with $\mathcal{H}_{\frac{1}{2+\alpha}}(0) = \frac{2^{\frac{1}{2+\alpha}}}{\Gamma(\frac{1+\alpha}{2+\alpha})}$ and the function $\mathbb{H}_\beta(w)$ given in Eq. (B2). For large z , we find that the scaling function decays as $\mathcal{F}_\alpha(z) \sim z^\alpha e^{-z^{2+\alpha}/4}$.

(2) We next calculate the probability distribution of the time $t_m(t)$ and show that it possesses the scaling structure

$$\mathcal{P}_m(t_m|t) = \frac{1}{t} \mathcal{G}_m^\alpha \left(\frac{t_m}{t} \right), \quad (10)$$

with the scaling function $\mathcal{G}_m^\alpha(z)$ defined as

$$\mathcal{G}_m^\alpha(z) = \frac{(2+\alpha)\mathcal{H}_{\frac{1}{2+\alpha}}(0)}{2z^{\frac{1+\alpha}{2+\alpha}}(1-z)^{\frac{1}{2+\alpha}}} \int_0^\infty dw \frac{\mathbb{X}_\alpha \left(\sqrt{\frac{1-z}{zw^{2+\alpha}}} \right)}{\mathcal{H}_{\frac{1}{2+\alpha}} \left(w^{\frac{2+\alpha}{2}} \right)}. \quad (11)$$

The functions $\mathcal{H}_\beta(x)$ and $\mathbb{X}_\beta(x)$ are defined, respectively, in Eqs. (23) and (B3). For BM, it follows from Eq. (2) that the scaling function $\mathcal{G}_m^\alpha(z)$ is symmetric under the transformation $z \rightarrow 1-z$. However, as evident from Eq. (11), this symmetry is no longer present for general α . This is further exemplified by the behavior of the scaling function as $z \rightarrow 0$ and $z \rightarrow 1$ for which we later show divergences of the form $\mathcal{G}_m^\alpha(z \rightarrow 0) \sim z^{-\frac{1+\alpha}{2+\alpha}}$ and $\mathcal{G}_m^\alpha(z \rightarrow 1) \sim (1-z)^{-\frac{1}{2}}$.

(3) We also compute the distribution $\mathcal{P}_r(t_r|t)$ of the residence time t_r for general α showing that it has the scaling form

$$\mathcal{P}_r(t_r|t) = \frac{1}{t} \mathcal{G}_r^\alpha \left(\frac{t_r}{t} \right), \quad (12)$$

where the scaling function $\mathcal{G}_r^\alpha(z)$ is given by

$$\mathcal{G}_r^\alpha(z) = \frac{\sin \left(\frac{\pi}{2+\alpha} \right)}{\pi [z(1-z)]^{\frac{1+\alpha}{2+\alpha}}} \times \frac{1}{z^{\frac{2}{2+\alpha}} + (1-z)^{\frac{2}{2+\alpha}} + 2 \cos \left(\frac{\pi}{2+\alpha} \right) [z(1-z)]^{\frac{1}{2+\alpha}}}. \quad (13)$$

This scaling function diverges as $\mathcal{G}_r^\alpha(z) \sim z^{-\frac{1+\alpha}{2+\alpha}}$ as $z \rightarrow 0$ and as $\mathcal{G}_r^\alpha(z) \sim (1-z)^{-\frac{1+\alpha}{2+\alpha}}$ as $z \rightarrow 1$.

(4) Finally, we derive the probability distribution $\mathcal{P}_\ell(t_\ell|t)$ of the last-passage time t_ℓ which also possesses the scaling structure

$$\mathcal{P}_\ell(t_\ell|t) = \frac{1}{t} \mathcal{G}_\ell^\alpha \left(\frac{t_\ell}{t} \right), \quad (14)$$

with the scaling function $\mathcal{G}_\ell^\alpha(z)$ given by

$$\mathcal{G}_\ell^\alpha(z) = \frac{z^{-\frac{1+\alpha}{2+\alpha}}(1-z)^{-\frac{1}{2+\alpha}}}{\Gamma\left(\frac{1+\alpha}{2+\alpha}\right)\Gamma\left(\frac{1}{2+\alpha}\right)}. \quad (15)$$

Here, once again, we find that the scaling function does not retain symmetry under the transformation $z \rightarrow 1-z$ for $\alpha \neq 0$. Consequently, we get different behaviors of $\mathcal{G}_\ell^\alpha(z)$ for $z \rightarrow 0$ and $z \rightarrow 1$, viz. $\mathcal{G}_\ell^\alpha(z \rightarrow 0) \sim z^{-\frac{1+\alpha}{2+\alpha}}$ and $\mathcal{G}_\ell^\alpha(z \rightarrow 1) \sim (1-z)^{-\frac{1}{2+\alpha}}$.

We remark that for $\alpha = 0$, all scaling functions written above converge to that of the BM in Eqs. (1) and (3). Also, note that the distributions of t_m, t_r , and t_ℓ are completely different for general α and they are identical only for $\alpha = 0$. Another interesting property contrary to that of the BM is that the distributions of t_m and t_ℓ for $\alpha \neq 0$ have asymmetric peaks (divergences) as $t_i \rightarrow 0^+$ and $t_i \rightarrow t^-$, where $t_i \in \{t_m, t_\ell\}$. All these observations exemplify that the properties of M, t_m, t_r ,

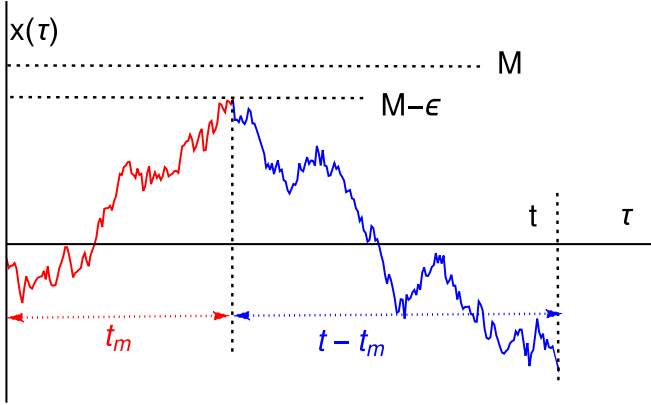


FIG. 2. Schematic of a typical trajectory of the particle in which it reaches $M - \epsilon$ at time t_m for the first time and remains below M in the remaining time $t - t_m$. The trajectory can be decomposed into two parts: from 0 to t_m (shown in red) and from t_m to t (shown in blue).

and t_ℓ for $\alpha \neq 0$ are remarkably different than that of the BM. In the following, we provide a detailed analysis of these quantities and point out the key differences for $\alpha \neq 0$.

III. EXTREME VALUE M AND TIME t_m TO REACH MAXIMUM

Let us begin with the joint distribution $\mathcal{P}(M, t_m|t)$ of the maximum displacement M and the time t_m at which the maximum is attained till duration t . The initial position is fixed to the origin. To compute this distribution, we decompose the trajectory in two parts: (i) the part from 0 to t_m and (ii) the part from t_m to t . They are shown schematically in Fig. 2, where the red half corresponds to part (i) and the blue half represents part (ii). Since the process is Markovian, the two parts are statistically independent.

Let us now calculate the contribution of each part. In part (i), the particle reaches $x = M$ at time t_m for the first time given that it was at the origin initially. Therefore, the probability weight in this part is just the first-passage time distribution $F_M(t_m|0)$ to reach M for the first time at t_m given that the particle was initially at $x = 0$. In part (ii), the process remains below $x = M$ in the interval $t - t_m$ such that it was at $x = M$ at time t_m . Hence, the weight of this part is given by the survival probability $S_M(t - t_m|M)$ where we have used the notation $S_{x_m}(\tau|x_0)$ to denote the probability that the particle has not crossed $x = x_m$ up to time τ starting from $x = x_0$. Note that the process remains below $x = M$ in both parts. As remarked before, these two contributions are statistically independent due to the Markovianity of the process. However, as shown later, it turns out that $S_M(\tau|M) = 0$ for all nonzero τ which implies that the contribution from part (ii) is zero. To circumvent this problem, we follow the procedure in [24,32] where we compute $F_{M-\epsilon}(t_m|0)$ and $S_M(t - t_m|M - \epsilon)$ instead of $F_M(t_m|0)$ and $S_M(t - t_m|M)$ and later take the $\epsilon \rightarrow 0^+$ limit. The joint distribution $\mathcal{P}(M, t_m|t)$ can then be written as

$$\mathcal{P}(M, t_m|t) = \frac{F_{M-\epsilon}(t_m|0)S_M(t - t_m|M - \epsilon)}{\mathcal{N}(\epsilon)}. \quad (16)$$

Here $1/\mathcal{N}(\epsilon)$ is the proportionality constant independent of t and t_m and fixed by the normalization condition. For later calculations, it turns out useful to take the double Laplace transformation of Eq. (16) with respect to $t_m (\rightarrow p)$ and $t (\rightarrow s)$:

$$\bar{P}(M, p|s) = \frac{\bar{F}_{M-\epsilon}(s + p|0)\bar{S}_M(s|M - \epsilon)}{\mathcal{N}(\epsilon)}, \quad (17)$$

where $\bar{P}(M, p|s)$ is the double Laplace transformation of $\mathcal{P}(M, t_m|t)$. Quite remarkably, using the Markovian property, we have completely specified the joint distribution of M and t_m in terms of its survival probability and first-passage time distribution. In what follows, we use the standard techniques to calculate these distributions and probabilities and then use Eq. (17) to compute the joint distribution.

A. Survival probability $S_M(t|x_0)$

Let us focus on the survival probability $S_M(t|x_0)$ for our model in Eq. (5). For simplicity, we consider $M \geq 0$ and $x_0 \leq M$ which is also consistent with our main aim of computing the joint distribution in Eq. (17). In the Ito setup, $S_M(t|x_0)$ obeys the backward Fokker-Planck equation [98]

$$\partial_t S_M(t|x_0) = D(x_0)\partial_{x_0}^2 S_M(t|x_0), \quad (18)$$

with $D(x_0)$ defined in Eq. (6). Our aim is to solve this equation for general α . In order to solve this equation, we have to specify the appropriate initial condition and boundary conditions. Initially, the particle starts from the position x_0 which is different from the position of the absorbing wall at $x = M$. Consequently, the particle always survives and we get

$$S_M(0|x_0) = 1. \quad (19)$$

Next, we specify the boundary conditions which read

$$S_M(t|x_0 \rightarrow M^-) = 0, \quad (20)$$

$$S_M(t|x_0 \rightarrow -\infty) = 1. \quad (21)$$

To understand the boundary condition in Eq. (20), note that if the particle initially starts from $x_0 \rightarrow M^-$, then it will immediately get absorbed. This results in the zero survival probability. On the other hand, if the particle is initially very far from the origin ($x_0 \rightarrow -\infty$), then it will survive the barrier at $x = M$ for all finite time. This gives rise to the second boundary condition in Eq. (21). Solving Eq. (18) [see Sec. I of the Supplemental Material (SM) [99] for details], we obtain the Laplace transformation of $S_M(t|x_0)$ for $x_0 \geq 0$ and $\alpha > -1$ as

$$\bar{S}_M(s|x_0) = \frac{1}{s} \left[1 - \frac{\mathcal{H}_{\frac{1}{2+\alpha}}((a_s x_0)^{\frac{2+\alpha}{2}})}{\mathcal{H}_{\frac{1}{2+\alpha}}((a_s M)^{\frac{2+\alpha}{2}})} \right], \quad (22)$$

where the functions $\mathcal{H}_\beta(x_0)$ and a_s are defined as

$$\mathcal{H}_\beta(x_0) = x_0^\beta [I_\beta(x_0) + I_{-\beta}(x_0)], \quad (23)$$

$$a_s = \left(\frac{s}{D_\alpha} \right)^{\frac{1}{2+\alpha}}, \quad \text{with } D_\alpha = \frac{D_0 l^\alpha (2 + \alpha)^2}{4}. \quad (24)$$

Here, $I_\beta(x_0)$ is the modified Bessel function of first kind. In the next section, we proceed to use the Laplace transform $\bar{S}_M(s|x_0)$ from Eq. (22) to calculate the joint distribution $\bar{P}(M, p|s)$ in Eq. (17).

B. Joint probability distribution $\mathcal{P}(M, t_m|t)$

Coming to the expression of $\bar{P}(M, p|s)$ in Eq. (17), we need to specify the Laplace transforms $\bar{S}_M(s|M - \epsilon)$ and $\bar{F}_{M-\epsilon}(s + p|0)$ in the limit $\epsilon \rightarrow 0^+$. Using Eq. (22), these Laplace transforms can be easily calculated. We refer to Eqs. (A1) and (A2) in Appendix A for the rigorous expression of these Laplace transforms. Plugging them into Eq. (17) gives $\bar{P}(M, p|s)$ as

$$\bar{P}(M, p|s) = \frac{\epsilon \mathcal{H}_{\frac{1}{2+\alpha}}(0)}{\mathcal{N}(\epsilon) s \mathcal{H}_{\frac{1}{2+\alpha}}((a_{s+p} M)^{\frac{2+\alpha}{2}})} \times \frac{\partial_M [\mathcal{H}_{\frac{1}{2+\alpha}}((a_s M)^{\frac{2+\alpha}{2}})]}{\mathcal{H}_{\frac{1}{2+\alpha}}((a_s M)^{\frac{2+\alpha}{2}})}. \tag{25}$$

The task now is to evaluate the function $\mathcal{N}(\epsilon)$. For this, we use the normalization condition of $\mathcal{P}(M, t_m|t)$ which in terms of the Laplace transform $\bar{P}(M, p|s)$ becomes

$$\int_0^\infty \bar{P}(M, p = 0|s) dM = \frac{1}{s}. \tag{26}$$

Plugging $\bar{P}(M, p = 0|s)$ from Eq. (25), it is easy to show that $\mathcal{N}(\epsilon) = \epsilon$. Substituting this in Eq. (25) yields

$$\bar{P}(M, p|s) = \frac{\mathcal{H}_{\frac{1}{2+\alpha}}(0)}{s \mathcal{H}_{\frac{1}{2+\alpha}}((a_{s+p} M)^{\frac{2+\alpha}{2}})} \times \frac{\partial_M [\mathcal{H}_{\frac{1}{2+\alpha}}((a_s M)^{\frac{2+\alpha}{2}})]}{\mathcal{H}_{\frac{1}{2+\alpha}}((a_s M)^{\frac{2+\alpha}{2}})}. \tag{27}$$

To summarize, we have exactly computed the Laplace transformation $\bar{P}(M, p|s)$ of the joint distribution of M and t_m for all values of α . To get the distribution in the time domain, one has to perform double inverse Laplace transformations which, unfortunately, turns out to be challenging. However, one could still obtain the explicit expressions of the marginal distributions of $M(t)$ and $t_m(t)$ by appropriately integrating $\bar{P}(M, p|s)$ in Eq. (27). In what follows, we use $\bar{P}(M, p|s)$ to obtain the marginal distribution of the maximum $M(t)$ followed by that of the arg-maximum $t_m(t)$.

C. Marginal distribution $P_m(M|t)$ of $M(t)$

To get the marginal distribution $P_m(M|t)$ of the maximum M , we integrate the joint distribution $\mathcal{P}(M, t_m|t)$ over all t_m . In terms of the Laplace variables p and s , this is equivalent to putting $p = 0$ in the expression of $\bar{P}(M, p|s)$ in Eq. (27) which then gives the Laplace transformation $\bar{P}_m(M|s)$ of the distribution $P_m(M|t)$. One finds

$$\begin{aligned} \bar{P}_m(M|s) &= \bar{P}(M, p = 0|s) \\ &= -\frac{d\bar{J}(M, s)}{dM}, \quad \text{with} \end{aligned} \tag{28}$$

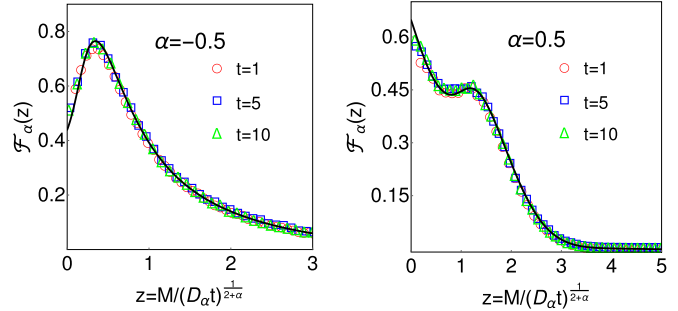


FIG. 3. Scaling function $\mathcal{F}_\alpha(z)$ in Eq. (9) is plotted for two values of α . In both panels, solid black line represents the analytic expression in Eq. (9) and the symbols represent simulation data. We have chosen $D_0 = 0.1$ and $l = 1$.

$$\bar{J}(M, s) = \frac{\mathcal{H}_{\frac{1}{2+\alpha}}(0)}{s \mathcal{H}_{\frac{1}{2+\alpha}}((a_s M)^{\frac{2+\alpha}{2}})}, \tag{29}$$

where the function $\mathcal{H}_\beta(x_0)$ in the last equation is defined in Eq. (23). We now proceed to perform the inverse Laplace transformation of $\bar{P}_m(M|s)$ in Eq. (28). Fortunately, this inversion can be exactly carried out. We refer to Sec. II of the SM [99] for the details of this calculation. The distribution $P_m(t_m|t)$ possesses the scaling structure as written in (8) with the scaling function $\mathcal{F}_\alpha(z)$ defined in (9).

A few remarks are in order. First, for $\alpha = 0$ in Eq. (9), we find that $\mathbb{H}_{\frac{1}{2}}(w)$ in Eq. (B2) has the simple form

$$\mathbb{H}_{\frac{1}{2}}(w) = \sqrt{\frac{2}{\pi}} \sin(w). \tag{30}$$

Plugging this in the expression of the scaling function $\mathcal{F}_\alpha(z)$ in (9) and performing the integration over w yields

$$\mathcal{F}_\alpha(z) = \frac{e^{-z^2/4}}{\sqrt{\pi}} \quad (\text{for } \alpha = 0). \tag{31}$$

This matches with the distribution of M for the standard Brownian motion in Eq. (1). However, for general α , the scaling function is given in Eq. (9). We also remark that the scaling of the maximum with time as $M \sim t^{\frac{1}{2+\alpha}}$ in Eq. (8) is quite expected since the position scales as $x \sim t^{\frac{1}{2+\alpha}}$. However, our analysis goes beyond this scaling behavior and also provides an exact form of the associated scaling function for all values of α .

In Fig. 3, we have plotted $\mathcal{F}_\alpha(z)$ and compared it against the simulation for two different values of α . For each value, we have conducted simulation for three different values of t . We see an excellent match of our analytic result in Eq. (9) with the simulations. To contrast these results with that of the standard Brownian motion, we look at the asymptotic behavior of $\mathcal{F}_\alpha(z)$ for different z . In particular, for $\alpha \neq 0$, we have shown in Sec. III of the SM [99] that the scaling function has the following asymptotic forms:

$$\mathcal{F}_\alpha(z) \simeq \frac{1}{C_\alpha \Gamma(\frac{1+\alpha}{2+\alpha})} - \frac{2z}{C_\alpha^2 \Gamma(\frac{\alpha}{2+\alpha})}, \quad \text{as } z \rightarrow 0, \tag{32}$$

$$\simeq \frac{(2 + \alpha) \mathcal{H}_{\frac{1}{2+\alpha}}(0)}{2^{\frac{3+2\alpha}{2+\alpha}}} z^\alpha e^{-\frac{z^2+\alpha}{4}}, \quad \text{as } z \rightarrow \infty, \tag{33}$$

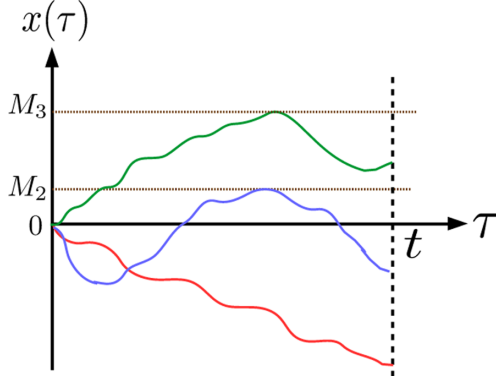


FIG. 4. Schematic of the trajectories that give rise to various values of the maximum M . For red trajectory, the particle stays below origin for all t . Consequently $M = 0$. Similarly, for blue and green trajectories, the values of maximum are $M_1 (\ll t^{\frac{1}{2+\alpha}})$ and $M_2 (\gg t^{\frac{1}{2+\alpha}})$, respectively.

where $C_\alpha = \frac{2^{2/2+\alpha} \Gamma(\frac{1}{2+\alpha})}{(2+\alpha) \Gamma(\frac{1+\alpha}{2+\alpha})}$. On the other hand for $\alpha = 0$, one gets from Eq. (31)

$$\mathcal{F}_0(z) \simeq \frac{1}{\sqrt{\pi}} \left(1 - \frac{z^2}{4} \right), \quad \text{as } z \rightarrow 0, \quad (34)$$

$$= \frac{e^{-z^2/4}}{\sqrt{\pi}}, \quad \text{as } z \rightarrow \infty. \quad (35)$$

We see that while, for $\alpha = 0$, the scaling function decreases quadratically with z as $z \rightarrow 0$, it changes linearly for $\alpha \neq 0$ [see Eq. (32)]. Also, the small- z behavior is rather different for $\alpha < 0$ and $\alpha > 0$. For $\alpha < 0$, we see, in Fig. 3 (left panel), that $\mathcal{F}_\alpha(z)$ rises initially with z , attains a maximum value, and then decreases again for large z . On the other hand, for $\alpha > 0$, we see that $\mathcal{F}_\alpha(z)$ initially decreases with z , then rises at some intermediate z until it attains a local maximum. After that, it again decreases for large z [see Fig. 3 (right panel)]. Quite interestingly, we see a nonmonotonic dependence of $\mathcal{F}_\alpha(z)$ on z for all $\alpha \neq 0$ (see Fig. 3). However, as illustrated in Eq. (31), the scaling function decreases monotonically with z for the BM for all values of z .

To understand the nonmonotonic nature of the scaling function $\mathcal{F}_\alpha(z)$, let us analyze the trajectories that give rise to different values of the maximum $M(t)$. For simplicity, we focus on $\alpha < 0$. In Fig. 4, we have shown a schematic illustration of three colored trajectories which contribute to three different maxima. The red trajectory stays below origin for all time which contributes to $M = 0$. On the other hand, the blue trajectory contributes nonzero $M_1 (\ll t^{\frac{1}{2+\alpha}})$. Since for $\alpha < 0$, the particle typically stays near the origin, it is more likely that it crosses the origin some number of times. Consequently, the likelihood of finding a red trajectory (where particle does not cross the origin) is less compared to a blue trajectory (where it crosses the origin a few times). In terms of the maximum M , this amounts to a smaller value of the distribution $P_m(M|t)$ for $M = 0$ as compared to the nonzero M [see Fig. 3 (left panel)]. However, to obtain large values of M , the fluctuations have to be sufficiently strong to take it far away from the origin on the positive side (see green trajectory in Fig. 4). Such fluctuations

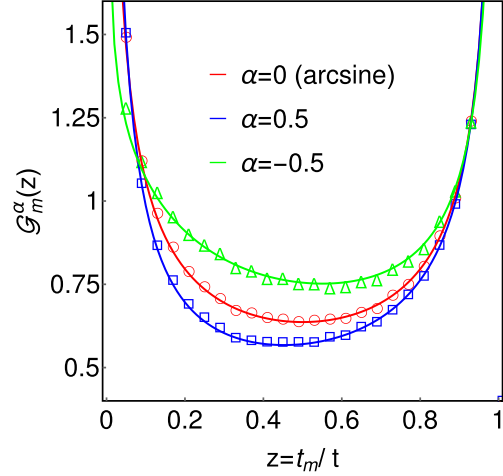


FIG. 5. We have plotted the scaling function $\mathcal{G}_m^\alpha(z)$ of arg-maximum t_m for three different values of α . The symbols represent the simulation data for $t = 5$ which are compared with the analytic expression (shown by solid line) in Eq. (11). Parameters chosen are $D_0 = 0.1$ and $l = 1$.

for $\alpha < 0$ are extremely rare which results in smaller values of the distribution $P_m(M|t)$ for large M . Overall, we obtain a nonmonotonic nature of $P_m(M|t)$ [or equivalently $\mathcal{F}_\alpha(z)$]. Although we have presented the physical reasoning for $\alpha < 0$, it is easy to extend it for $\alpha > 0$ also.

D. Marginal distribution $\mathcal{P}_m(t_m|t)$ of $t_m(t)$

This section deals with the probability distribution $\mathcal{P}_m(t_m|t)$ of the arg-maximum t_m . Let us denote its double Laplace transformation by $\bar{\mathcal{P}}_m(p|s)$. Marginalizing $\bar{\mathcal{P}}(M, p|s)$ in Eq. (27) by integrating over all M , we find

$$\begin{aligned} \bar{\mathcal{P}}_m(p|s) &= \int_0^\infty dM \frac{\mathcal{H}_{\frac{1}{2+\alpha}}(0)}{s \mathcal{H}_{\frac{1}{2+\alpha}}((a_s+p)M^{\frac{2+\alpha}{2}})} \\ &\times \frac{\partial_M [\mathcal{H}_{\frac{1}{2+\alpha}}((a_s M)^{\frac{2+\alpha}{2}})]}{\mathcal{H}_{\frac{1}{2+\alpha}}((a_s M)^{\frac{2+\alpha}{2}})}. \end{aligned} \quad (36)$$

Recall that the function $\mathcal{H}_\beta(x_0)$ is defined in Eq. (23). To get the distribution in the time domain, one then needs to perform the double inverse Laplace transformation of Eq. (36). In Sec. IV of the SM [99], we have explicitly carried out this inversion. The final form of the distribution shows that $\mathcal{P}_m(t_m|t)$ possesses the scaling form as quoted in Eq.(10) where the scaling function $\mathcal{G}_m^\alpha(z)$ is given in Eq. (11).

In Fig. 5, we have illustrated this scaling behavior for different values of α . For all values, we see excellent agreement of our analytic results with the numerical simulations. To recover the arcsine law for $\alpha = 0$, we notice that $\mathbb{X}_\alpha(x) = \pi^{-1}$ from Eq. (B3) and $\mathcal{H}_{\frac{1}{2}}(x) = \sqrt{\frac{2}{\pi}} e^x$ from Eq. (23). Plugging

these forms in the expression of $\mathcal{G}_m^\alpha(z)$ in Eq. (11) and performing the integration over w , we get

$$\mathcal{G}_m^\alpha(z) = \frac{1}{\pi \sqrt{z(1-z)}} \quad (\text{for } \alpha = 0),$$

which matches with the arcsine law in Eq. (2). Curiously, the scaling function $\mathcal{G}_m^\alpha(z)$ is symmetric under the transformation $z \rightarrow 1-z$ only for $\alpha = 0$. On the other hand, for nonzero α , we see that $\mathcal{G}_m^\alpha(z)$ is not symmetric under this transformation. This is also exemplified in Fig. 5. To see this clearly, let us look at the form of $\mathcal{G}_m^\alpha(z)$ for $z \rightarrow 0$ and $z \rightarrow 1$. For general α , we find (see Sec. V of the SM [99]) that the scaling function diverges as $\mathcal{G}_m^\alpha(z \rightarrow 0) \sim z^{-\frac{1+\alpha}{2+\alpha}}$ and $\mathcal{G}_m^\alpha(z \rightarrow 1) \sim (1-z)^{-\frac{1}{2}}$. Clearly, the divergences at two ends of z are asymmetric for all $\alpha \neq 0$. Surprisingly, the divergence of the scaling function as $z \rightarrow 1$ is completely universal, characterized by an α -independent exponent $1/2$. The prefactor, however, may depend on the value of α as illustrated in Sec. V of the SM [99]. Heuristically, this α -independence divergence can be understood as follows: From Eq. (16), we see that the joint distribution $\mathcal{P}(M, t_m|t)$ is proportional to the survival probability $S_M(t - t_m|M - \epsilon)$ which for $t_m \rightarrow t^-$ scales as $S_M(t - t_m|M - \epsilon) \sim (t - t_m)^{-1/2}$ for all values of α [via Eq. (A1)]. Consequently, the marginal distribution $\mathcal{P}_m(t_m|t)$ also diverges as $(t - t_m)^{-1/2}$ for all values of α .

IV. RESIDENCE TIME DISTRIBUTION $\mathcal{P}_r(t_r|t)$

Residence time refers to the amount of time that the particle spends in the $x > 0$ region till duration t . Formally, it is defined as $t_r(t) = \int_0^t d\tau \Theta(x(\tau))$, where $\Theta(x)$ denotes the Heaviside theta function. For standard Brownian motion, the distribution of t_r is given in Eq. (3). This expression reveals that the distribution peaks (diverges) as $t_r \rightarrow 0^+$ and $t_r \rightarrow t^-$, whereas it exhibits minimum value at $t_r = t/2$. This implies rather a counter-intuitive property of the Brownian motion where once it crosses the origin on positive or negative side, it is reluctant to come back [73]. A natural question is, what happens to this property for general α ? In order to answer this question, we look at the residence time distribution for general α in this section.

Let us denote the distribution of t_r by $\mathcal{P}_r(t_r, x_0|t)$ where x_0 is the initial position and t is the total observation time. We later take $x_0 = 0$. Denoting the Laplace transformation of $\mathcal{P}_r(t_r, x_0|t)$ with respect to t_r as $\mathcal{Q}(p, x_0|t)$, we have

$$\mathcal{Q}(p, x_0|t) = \langle e^{-pt_r} \rangle \quad (37)$$

$$= \int_0^\infty dt_r e^{-pt_r} \mathcal{P}_r(t_r, x_0|t). \quad (38)$$

The Laplace transform $\mathcal{Q}(p, x_0|t)$ satisfies the following backward master equations [73]:

$$\partial_t \mathcal{Q}(p, x_0|t) = [D(x_0) \partial_{x_0}^2 - p \Theta(x_0)] \mathcal{Q}(p, x_0|t), \quad (39)$$

where $D(x_0)$ is defined in Eq. (6). In order to solve this equation, we need to specify the appropriate initial and boundary conditions. For initial condition, we note that if $t \rightarrow 0$, then the residence time t_r also tends to zero, i.e., $t_r \rightarrow 0$. Using this in Eq. (37), we obtain

$$\mathcal{Q}(p, x_0|t \rightarrow 0) = 1. \quad (40)$$

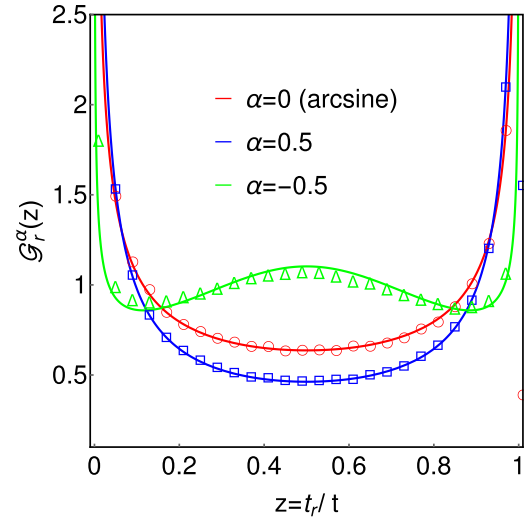


FIG. 6. Scaling function $\mathcal{G}_r^\alpha(z)$ in Eq. (13) for the occupation time distribution is plotted and compared with the numerical simulation for three different values of α . The analytic expression in Eq. (13) is shown in solid line and the simulation data are shown by symbols. We have chosen $D_0 = 0.1$, $l = 1$, and $t = 5$.

On the other hand, for any finite t , we have the following boundary conditions:

$$\mathcal{Q}(p, x_0 \rightarrow -\infty|t) = 1, \quad (41)$$

$$\mathcal{Q}(p, x_0 \rightarrow \infty|t) = e^{-pt}. \quad (42)$$

Note that the first boundary condition follows from the fact that if $x_0 \rightarrow -\infty$, then the particle essentially stays in the $x < 0$ region for all finite t . Consequently $t_r = 0$ which from Eq. (37) leads to $\mathcal{Q}(p, x_0 \rightarrow -\infty|t) = 1$. On the other hand, if $x_0 \rightarrow \infty$, then the particle stays in $x > 0$ region for all finite t and $t_r = t$. Plugging this in Eq. (37) results in the second boundary condition in Eq. (42).

We now proceed to solve the backward equation (39) with these initial and boundary conditions. To this aim, we take another Laplace transformation of $\mathcal{Q}(p, x_0|t)$ with respect to t and denote it by $\bar{\mathcal{Q}}(p, x_0|s)$. One can then appropriately transform the backward equation in terms of $\bar{\mathcal{Q}}(p, x_0|s)$ and solve it. To maintain continuity of the presentation, we have relegated these details to Sec. VI of the SM [99]. The final solution for $x_0 = 0$ reads

$$\bar{\mathcal{Q}}(p|s) = \frac{1}{s} - \frac{p}{s(s+p)} \left[1 + \left(\frac{s}{s+p} \right)^{\frac{1}{2+\alpha}} \right]^{-1}, \quad (43)$$

where we have used the short-hand notation $\bar{\mathcal{Q}}(p|s) = \bar{\mathcal{Q}}(p, x_0 = 0|s)$. One now has to perform the double inverse Laplace transformation of $\bar{\mathcal{Q}}(p|s)$ to get the distribution in the time domain. Fortunately, this inversion can be performed for all $\alpha > -1$ [82,90]. The distribution $\mathcal{P}_r(t_r|t)$ indeed has the scaling form in Eq. (12) and the scaling function $\mathcal{G}_r^\alpha(z)$ is given in Eq. (13).

For $\alpha = 0$, we recover the arcsine law in Eq. (3) for distribution $\mathcal{P}_r(t_r|t)$ in Eq. (12). In Fig. 6, we have illustrated the scaling function $\mathcal{G}_r^\alpha(z)$ for three different values of α and

compared it against the simulation. We find excellent agreement between them. Contrary to the arg-maximum $t_m(t)$, we see that $\mathcal{G}_r^\alpha(z)$ is symmetric about $z = \frac{1}{2}$ for all values of α . In fact, from Eq. (13), we see that it diverges as $z^{-\frac{1+\alpha}{2+\alpha}}$ and $(1-z)^{-\frac{1+\alpha}{2+\alpha}}$ as $z \rightarrow 0$ and $z \rightarrow 1$ respectively. Interestingly, in Fig. 6, we see that the scaling function exhibits local maxima at $z = 1/2$ for $\alpha = -0.5$ which is in contrast to the other two values of α for which one finds minima at $z = 1/2$. To understand this behavior, we analyze $\mathcal{G}_r^\alpha(z)$ in the vicinity of $z = 1/2$. Expanding $\mathcal{G}_r^\alpha(z)$ in Eq. (13) for $z = \frac{1+\bar{\epsilon}}{2}$ with $\bar{\epsilon} \rightarrow 0$, we get

$$\mathcal{G}_r^\alpha\left(\frac{1+\bar{\epsilon}}{2}\right) \simeq \frac{2}{\pi} \tan\left(\frac{\pi}{2(2+\alpha)}\right) + \frac{\mathbb{K}(\alpha)\bar{\epsilon}^2}{2\pi}, \quad (44)$$

where the function $\mathbb{K}(\alpha)$ is defined as

$$\mathbb{K}(\alpha) = \frac{[2 + \alpha(4 + \alpha) + (2 + \alpha)^2 \cos\left(\frac{\pi}{2+\alpha}\right)]}{(2 + \alpha)^2 \sin^{-1}\left(\frac{\pi}{2+\alpha}\right) \sec^{-4}\left(\frac{\pi}{2(2+\alpha)}\right)}. \quad (45)$$

Now, $\mathcal{G}_r^\alpha(z)$ will exhibit local maxima or minima at $z = 1/2$ depending on whether $\mathbb{K}(\alpha)$ is positive or negative. Defining the critical value of α as

$$\mathbb{K}(\alpha_c) = 0 \Rightarrow \alpha_c \simeq -0.3182, \quad (46)$$

we find that $\mathbb{K}(\alpha) > 0$ for $\alpha \geq \alpha_c$ and $\mathbb{K}(\alpha) < 0$ for $\alpha < \alpha_c$. Therefore, we expect a local maxima at $z = 1/2$ for the scaling function $\mathcal{G}_r^\alpha(z)$ for $\alpha < \alpha_c$. Quite remarkably, this implies that for $\alpha \geq \alpha_c$, the particle, starting from the origin, typically stays entirely on the positive side or entirely on the negative side. The paths in which the particle spends equal amounts of time on the positive and negative sides are relatively rare. This ‘‘stiff’’ property (or reluctance to cross the origin) has been long known for BM [73]. Here, we have shown that it gets extended for all $\alpha \geq \alpha_c$. On the other hand, for $\alpha < \alpha_c$, this ‘‘stiffness’’ is reduced which results in the local maximum of $\mathcal{G}_r^\alpha(z)$ at $z = 1/2$. In fact, as $\alpha \rightarrow -1^+$, the scaling function simply becomes $\delta(z - 1/2)$. This implies that the particle typically spends equal amounts of time on the positive and negative sides of the origin which is in sharp contrast to the standard Brownian motion.

V. LAST-PASSAGE TIME DISTRIBUTION $\mathcal{P}_\ell(t_\ell|t)$

We now study the probability distribution $\mathcal{P}_\ell(t_\ell|t)$ of time t_ℓ that the particle crosses the origin for the last time till duration t . As illustrated in Fig. 1, we can analyze this problem by decomposing the trajectory into two parts. In the first part, the particle reaches the origin at time t_ℓ after starting its motion initially from the origin. The weight of this part is just the free probability distribution $\mathbb{P}(0, t_\ell|0)$. In the second part, the particle does not cross the origin in the remaining time interval $(t - t_\ell)$ given that it was at the origin at time t_ℓ . Then, the contribution of this part to $\mathcal{P}_\ell(t_\ell|t)$ is the survival probability $S_0(t - t_\ell|0)$. Since the process is Markovian, these two contributions are statistically independent.

However, one encounters a similar problem as encountered for the case of extreme value statistics in Sec. III. Recall from this analysis of extreme value statistics that $S_0(t - t_\ell|0)$ is exactly equal to zero for all $t - t_\ell$. In order to circumvent this problem, we instead compute the quantities $\mathbb{P}(\epsilon, t_\ell|0)$

and $S_0(t - t_\ell|\epsilon)$ and take the $\epsilon \rightarrow 0^+$ limit at an appropriate stage of the calculation. Then, the distribution $\mathcal{P}_\ell(t_\ell|t)$ can be written as

$$\mathcal{P}_\ell(t_\ell|t) = \frac{\mathbb{P}(\epsilon, t_\ell|0)S_0(t - t_\ell|\epsilon)}{\mathcal{N}_L(\epsilon)}, \quad (47)$$

where the function $\mathcal{N}_L(\epsilon)$ is just the normalization factor. It is instructive to take the double Laplace transformation of this equation with respect to $t_\ell (\rightarrow p)$ and $t (\rightarrow s)$ to get

$$\bar{\mathcal{P}}_\ell(p|s) = \frac{\bar{\mathbb{P}}(\epsilon, s+p|0)\bar{S}_0(s|\epsilon)}{\mathcal{N}_L(\epsilon)}. \quad (48)$$

In this equation, we have used the notation $\bar{\mathcal{P}}_\ell(p|s)$ and $\bar{\mathbb{P}}(\epsilon, s|0)$ to denote the Laplace transform of $\mathcal{P}_\ell(t_\ell|t)$ and $\mathbb{P}(\epsilon, t|0)$, respectively. Interestingly, Eq. (48) implies that the problem of the last-passage time has now been reduced to the problem of computing survival probability and distribution in an infinite line. The Laplace transforms $\bar{\mathbb{P}}(\epsilon, s|0)$ and $\bar{S}_0(s|\epsilon)$ can be explicitly obtained (see Sec. VII of the SM [99] for details) to be

$$\bar{\mathbb{P}}(\epsilon, s|0) \simeq \frac{\mathcal{A}_L(\epsilon)}{s^{\frac{1}{2+\alpha}}}, \quad (49)$$

$$\bar{S}_0(s|\epsilon) \simeq \frac{\mathcal{B}_L(\epsilon)}{s^{\frac{1+\alpha}{2+\alpha}}}, \quad (50)$$

where $\mathcal{A}_L(\epsilon)$ and $\mathcal{B}_L(\epsilon)$ are functions of ϵ whose explicit forms are given, respectively, in Eqs. (S105) and (S107) of the SM [99]. Next, we insert Eqs. (49) and (50) in Eq. (48) to write $\bar{\mathcal{P}}_\ell(p|s)$ as

$$\bar{\mathcal{P}}_\ell(p|s) \simeq \frac{\mathcal{A}_L(\epsilon)\mathcal{B}_L(\epsilon)}{\mathcal{N}_L(\epsilon)} \frac{1}{s^{\frac{1+\alpha}{2+\alpha}}(s+p)^{\frac{1}{2+\alpha}}}. \quad (51)$$

We now have to specify the normalization factor $\mathcal{N}_L(\epsilon)$. To evaluate this factor, we use the normalization condition $\bar{\mathcal{P}}_\ell(0|s) = 1/s$ from which it is easy to show that $\mathcal{N}_L(\epsilon) = \mathcal{A}_L(\epsilon)\mathcal{B}_L(\epsilon)$. This leads us to write $\bar{\mathcal{P}}_\ell(p|s)$ as

$$\bar{\mathcal{P}}_\ell(p|s) = \frac{1}{s^{\frac{1+\alpha}{2+\alpha}}(s+p)^{\frac{1}{2+\alpha}}}. \quad (52)$$

Finally, performing the double inverse Laplace transformation of this equation, we find that the distribution $\mathcal{P}_\ell(t_\ell|t)$ of the last-passage time t_ℓ , for $\alpha > -1$, indeed possesses the scaling behavior of Eq. (14) with the scaling function $\mathcal{G}_\ell^\alpha(z)$ defined in Eq. (15) for general α . In Fig. 7, we have plotted $\mathcal{G}_\ell^\alpha(z)$ for three values of α and compared against the numerical simulations. We observe an excellent match for all α .

One again, we see from Eq. (15) that $\mathcal{G}_\ell^\alpha(z)$ possesses $z \rightarrow 1 - z$ symmetry only for $\alpha = 0$. However, the symmetry is absent for nonzero values for α as elucidated in Fig. 7. Consequently, we get different divergences of the scaling function at the two ends, i.e., $\mathcal{G}_\ell^\alpha(z \rightarrow 0) \sim z^{-\frac{1+\alpha}{2+\alpha}}$ and $\mathcal{G}_\ell^\alpha(z \rightarrow 1) \sim (1 - z)^{-\frac{1}{2+\alpha}}$. Physically, this asymmetric nature can be understood in the following way: For $\alpha > 0$, the particle typically stays away from the origin due to the large values of the diffusion coefficient around the origin. This gives rise to the smaller values of t_ℓ . As a result, the distribution $\mathcal{P}_\ell(t_\ell|t)$ is sharply peaked at the smaller values of t_ℓ . On the other hand, for $\alpha < 0$, the particle typically stays near the origin which

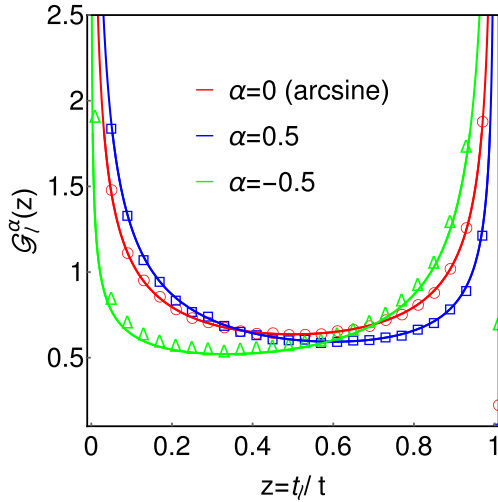


FIG. 7. Scaling function $\mathcal{G}_\ell^\alpha(z)$ in Eq. (15) for the last passage time distribution is plotted and compared with the numerical simulation for three different values of α . The analytic expression in Eq. (15) is shown in solid line and the simulation data are shown by symbols. We have chosen $D_0 = 0.1$, $l = 1$, and $t = 5$.

enhances its chances to cross the origin. This essentially gives rise to the large values of t_ℓ and peaking of $\mathcal{P}_\ell(t_\ell|t)$ at these values.

VI. CONCLUSION

To conclude, we have studied a model of anomalous diffusion in which a single particle moves in a one-dimensional heterogeneous medium with a spatially varying diffusion coefficient of the form $D(x) \sim |x|^{-\alpha}$ with $\alpha > -1$. Depending on the exponent α , this model displays superdiffusive ($-1 < \alpha < 0$), diffusive ($\alpha = 0$), or subdiffusive ($0 < \alpha < \infty$) scaling of the mean-squared displacement (MSD). Curiously, this simple Markov process also exhibits weak ergodicity breaking in the sense that the time averaged and ensemble averaged MSDs are not equal even at large times [10–16].

In this paper, we extensively investigated the statistical properties of the maximum displacement $M(t)$ and time $t_m(t)$ taken to reach this maximum till duration t . Exploiting the path decomposition technique for Markov processes [24], we derived, for all α , the joint probability distribution of $M(t)$ and $t_m(t)$. Marginalizing this joint distribution for $M(t)$ shows that the distribution $P_m(M|t)$ possesses scaling behavior in $M/t^{\frac{1}{2+\alpha}}$ with the corresponding scaling function $\mathcal{F}_\alpha(z)$ rigorously derived in Eq. (9). Contrary to the standard Brownian motion (BM), we obtain that $\mathcal{F}_\alpha(z)$, for nonzero α , has a nonmonotonic dependence on z which is a consequence of the heterogeneity in the environment. The behavior of $\mathcal{F}_\alpha(z)$ for $\alpha < 0$ and $\alpha > 0$ is also rather different. For $\alpha < 0$, the scaling function rises initially for small z , attains a maximum value, and then decays for large z . On the other hand, for $\alpha > 0$, it initially decreases with z then rises at some intermediate z until it attains a local maximum. After that, it again decreases for large z . This behavior has been illustrated in Fig. 3.

Our analysis on extreme value statistics also provides an exact expression of the marginal distribution $\mathcal{P}_m(t_m|t)$ of the arg-maximum $t_m(t)$ in Eq. (10). In contrast to the BM, we find that the distribution $\mathcal{P}_m(t_m|t)$, for $\alpha \neq 0$, is not symmetric about $t_m = t/2$. This difference is also exemplified by asymmetric peaks (divergences) of $\mathcal{P}_m(t_m|t)$ as $t_m \rightarrow 0^+$ and $t_m \rightarrow t^-$, namely, $\mathcal{P}_m(t_m \rightarrow 0|t) \sim t_m^{-\frac{1+\alpha}{2+\alpha}}$ and $\mathcal{P}_m(t_m \rightarrow t|t) \sim (t - t_m)^{-\frac{1}{2}}$. Recall that for BM, $\mathcal{P}_m(t_m|t)$ is symmetric about $t_m = t/2$ and diverges identically as $\mathcal{P}_m(t_m \rightarrow 0|t) \sim t_m^{-\frac{1}{2}}$ and $\mathcal{P}_m(t_m \rightarrow t|t) \sim (t - t_m)^{-\frac{1}{2}}$.

The second part of our paper dealt with the analysis of the residence time $t_r(t)$ for which we computed the probability distribution $\mathcal{P}_r(t_r|t)$ exactly for all values of α . Quite remarkably, we find the existence of a critical α (which we denote by $\alpha_c = -0.3182$) such that $\mathcal{P}_r(t_r|t)$ has minima at $t_r = t/2$ for $\alpha \geq \alpha_c$ whereas it exhibits local maximum at $t_r = t/2$ for $\alpha < \alpha_c$. We also provided a simple physical reasoning of this behavior based on the likelihood of the particle to stay on one side of the origin. The appearance of local maxima at $t_r = t/2$ is in sharp contrast to the standard BM. Finally, we calculated the distribution $\mathcal{P}_\ell(t_\ell|t)$ of the last-passage time $t_\ell(t)$ and showed that it is also asymmetric about $t_\ell(t) = t/2$ for nonzero α . This is further illustrated by the difference in behavior of $\mathcal{P}_\ell(t_\ell|t)$ as $t_\ell \rightarrow 0^+$ and $t_\ell \rightarrow t^-$, viz. $\mathcal{P}_\ell(t_\ell \rightarrow 0|t) \sim t_\ell^{-\frac{1+\alpha}{2+\alpha}}$ and $\mathcal{P}_\ell(t_\ell \rightarrow t|t) \sim (t - t_\ell)^{-\frac{1}{2+\alpha}}$. We emphasize that while the distributions of $t_m(t)$, $t_r(t)$, and $t_\ell(t)$ are all identical to Eq. (3) for $\alpha = 0$, they turn out to be significantly different for $\alpha \neq 0$. In fact, for $\alpha = 0$ (BM), the equivalence between $t_m(t)$ and $t_\ell(t)$ can be established based on the reflection property, inversion symmetry, and time-reversal symmetry [100]. However, these symmetries are not present for $\alpha \neq 0$ which results in inequivalence between $t_m(t)$ and $t_\ell(t)$.

Here, we have showcased a simple example of a heterogeneous diffusion model driven by white Gaussian noise for which we could derive many results on extremal statistics and path functionals exactly. Unraveling these results for other complex heterogeneous models remains a promising future direction. Recently heterogeneous diffusion processes driven by colored noise have garnered significant interest due to their potential application in biological systems [18–20]. It would be interesting to see how our results get modified in these scenarios. Another interesting direction is to explore the ramifications of the combined effect of HDP and other models like fractional Brownian motion [21,37,38,101] and scaled Brownian motion [22] on the extreme value statistics and arcsine laws.

Finally, we remark that our work may be verified in experiments involving diffusion of tracer proteins in the cytoplasmic part of the cell where substantial heterogeneity arises due to the nonuniform distribution of various crowding obstacles such as ribosomes, nuclei acids, and cytoskeletons [1]. The space-dependent diffusion coefficient is also observed in experiments involving particles trapped between two nearly parallel plates [4]. It would be interesting to compare our analytical results with these experiments.

ACKNOWLEDGMENTS

I am indebted to my supervisor Dr. Anupam Kundu for collaboration on other projects upon which the current work is based. I acknowledge support of the Department of Atomic Energy, Government of India, under Project No. 12-R&D-TFR-5.10-1100.

APPENDIX A: DERIVATION OF $\bar{P}(M, p|s)$ IN EQUATION (17)

Here, we derive the expression of the Laplace transform $\bar{P}(M, p|s)$ of joint distribution in Eq. (25). From Eq. (17), we see that this reduces to the problem of computing $\bar{S}_M(s|M - \epsilon)$ and $\bar{F}_{M-\epsilon}(s + p|0)$. Using Eq. (22), we get

$$\bar{S}_M(s|M - \epsilon) \simeq \frac{\epsilon \partial_M [\mathcal{H}_{\frac{1}{2+\alpha}}((a_s M)^{\frac{2+\alpha}{2}})]}{s \mathcal{H}_{\frac{1}{2+\alpha}}((a_s M)^{\frac{2+\alpha}{2}})}, \quad (\text{A1})$$

$$\begin{aligned} \bar{F}_{M-\epsilon}(s + p|0) &= 1 - (s + p) \bar{S}_{M-\epsilon}(s + p|0) \\ &\simeq \frac{\mathcal{H}_{\frac{1}{2+\alpha}}(0)}{\mathcal{H}_{\frac{1}{2+\alpha}}((a_{s+p} M)^{\frac{2+\alpha}{2}})}. \end{aligned} \quad (\text{A2})$$

Finally, inserting Eqs. (A1) and (A2) in Eq. (17) results in

$$\begin{aligned} \bar{P}(M, p|s) &= \frac{\epsilon \mathcal{H}_{\frac{1}{2+\alpha}}(0)}{\mathcal{N}(\epsilon) s \mathcal{H}_{\frac{1}{2+\alpha}}((a_{s+p} M)^{\frac{2+\alpha}{2}})} \\ &\times \frac{\partial_M [\mathcal{H}_{\frac{1}{2+\alpha}}((a_s M)^{\frac{2+\alpha}{2}})]}{\mathcal{H}_{\frac{1}{2+\alpha}}((a_s M)^{\frac{2+\alpha}{2}})}. \end{aligned} \quad (\text{A3})$$

This result has been quoted in Eq. (25).

APPENDIX B: IMPORTANT FORMULAE

We present here a list of the expressions and the notations that we have used in our paper:

$$\mathcal{H}_\beta(w) = w^\beta [I_\beta(w) + I_{-\beta}(w)], \quad (\text{B1})$$

$$\mathbb{H}_\beta(w) = \frac{1}{2\pi\beta i} \left[\frac{1}{\mathcal{H}_\beta(-iw)} - \frac{1}{\mathcal{H}_\beta(iw)} \right]. \quad (\text{B2})$$

$$\mathbb{X}_\alpha(w) = \frac{e^{-\frac{i\pi}{2+\alpha}}}{2\pi i} \left[\frac{\mathcal{H}_{\frac{1+\alpha}{2+\alpha}}(\frac{i}{w})}{\mathcal{H}_{\frac{1}{2+\alpha}}(\frac{i}{w})} - \frac{e^{-\frac{2i\pi}{2+\alpha}} \mathcal{H}_{\frac{1+\alpha}{2+\alpha}}(-\frac{i}{w})}{\mathcal{H}_{\frac{1}{2+\alpha}}(-\frac{i}{w})} \right]. \quad (\text{B3})$$

-
- [1] T. Kühn, T. O. Ihalainen, J. Hyväluoma, N. Dross, S. F. Willman, J. Langowski, M. Vihinen-Ranta, and J. Timonen, Protein diffusion in mammalian cell cytoplasm, *PLoS ONE* **6**, e22962 (2011).
- [2] B. P. English, V. Hauryliuk, A. Sanamrad, S. Tankov, N. H. Dekker, and J. Elf, Single-molecule investigations of the stringent response machinery in living bacterial cells, *Proc. Natl. Acad. Sci. USA* **108**, E365 (2011).
- [3] M. Platani, I. Goldberg, A. I. Lamond and J. R. Swedlow, Cajal body dynamics and association with chromatin are ATP-dependent, *Nat. Cell Biol.* **4**, 502 (2002).
- [4] P. Lançon, G. Batrouni, L. Lobry and N. Ostrowsky, Drift without flux: Brownian walker with a space-dependent diffusion coefficient, *Eur. Phys. Lett.* **54**, 28 (2001).
- [5] M. Yanga and M. Ripoll, Drift velocity in non-isothermal inhomogeneous systems, *J. Chem. Phys.* **136**, 204508 (2012).
- [6] J. J. Erik Maris, D. Fu, F. Meirer and B. M. Weckhuysen, Single-molecule observation of diffusion and catalysis in nanoporous solids, *Adsorption* **27**, 423 (2021).
- [7] J. Mittal, T. M. Truskett, J. R. Errington and G. Hummer, Layering and Position-Dependent Diffusive Dynamics of Confined Fluids, *Phys. Rev. Lett.* **100**, 145901 (2008).
- [8] L. F. Richardson, Atmospheric diffusion shown on a distance-neighbour graph, *Proc. R. Soc. London, Ser. A* **110**, 709 (1926).
- [9] B. O'Shaughnessy and I. Procaccia, Analytical Solutions for Diffusion on Fractal Objects, *Phys. Rev. Lett.* **54**, 455 (1985).
- [10] A. G. Cherstvy and R. Metzler, Population splitting, trapping, and non-ergodicity in heterogeneous diffusion processes, *Phys. Chem. Chem. Phys.* **15**, 20220 (2013).
- [11] A. G. Cherstvy, A. V. Chechkin and R. Metzler, Particle invasion, survival, and non-ergodicity in 2D diffusion processes with space-dependent diffusivity, *Soft Matter* **10**, 1591 (2014).
- [12] N. Leibovich and E. Barkai, Infinite ergodic theory for heterogeneous diffusion processes, *Phys. Rev. E* **99**, 042138 (2019).
- [13] X. Wang, W. Deng and Y. Chen, Ergodic properties of heterogeneous diffusion processes in a potential well, *J. Chem. Phys.* **150**, 164121 (2019).
- [14] K. S. Fa and E. K. Lenzi, Anomalous diffusion, solutions and first passage time: Influence of diffusion coefficient, *Phys. Rev. E* **71**, 012101 (2005).
- [15] A. G. Cherstvy and R. Metzler, Ergodicity breaking and particle spreading in noisy heterogeneous diffusion processes, *J. Chem. Phys.* **142**, 144105 (2015).
- [16] W. Wang, A. G. Cherstvy, H. Kantz, R. Metzler, and I. M. Sokolov, Time averaging and emerging nonergodicity upon resetting of fractional Brownian motion and heterogeneous diffusion processes, *Phys. Rev. E* **104**, 024105 (2021).
- [17] P. Singh, S. Sabhapandit, and A. Kundu, Run-and-tumble particle in inhomogeneous media in one dimension, *J. Stat. Mech.* (2020) 083207.
- [18] N. M. Mutohya, Y. Xu, Y. Li, and R. Metzler, Characterising stochastic motion in heterogeneous media driven by coloured non-Gaussian noise, *J. Phys. A: Math. Theor.* **54**, 295002 (2021).
- [19] Y. Xu, X. Liu, Y. Li, and R. Metzler, Heterogeneous diffusion processes and nonergodicity with Gaussian colored noise in layered diffusivity landscapes, *Phys. Rev. E* **102**, 062106 (2020).
- [20] N. M. Mutohya, Y. Xu, Y. Li, R. Metzler, and N. M. Mutua, First passage dynamics of stochastic motion in heterogeneous media driven by correlated white Gaussian and coloured non-Gaussian noises, *J. Phys. Complex.* **2**, 045012 (2021).
- [21] W. Wang, A. G. Cherstvy, X. Liu, and R. Metzler, Anomalous diffusion and nonergodicity for heterogeneous diffusion

- processes with fractional Gaussian noise, *Phys. Rev. E* **102**, 012146 (2020).
- [22] A. G. Cherstvy and R. Metzler, Ergodicity breaking, ageing, and confinement in generalized diffusion processes with position and time dependent diffusivity, *J. Stat. Mech.* (2015) P05010.
- [23] P. Lévy, On certain homogeneous stochastic processes, *Compositio Mathematica* **7**, 283 (1940).
- [24] S. N. Majumdar, J. Randon-Furling, M. J. Kearney, and M. Yor, On the time to reach maximum for a variety of constrained Brownian motions, *J. Phys. A: Math. Theor.* **41**, 365005 (2008).
- [25] P. Singh and A. Pal, Extremal statistics for stochastic resetting systems, *Phys. Rev. E* **103**, 052119 (2021).
- [26] F. Mori, S. N. Majumdar, and G. Schehr, Distribution of the time of the maximum for stationary processes, *Eur. Phys. Lett.* **135**, 30003 (2021).
- [27] G. Schehr and S. N. Majumdar, Exact record and order statistics of random walks via first-passage ideas, in *First-Passage Phenomena and Their Applications*, edited by R. Metzler, G. Oshani, and S. Redner (World Scientific Publishing Co., Singapore, 2014), p. 226.
- [28] G. Schehr, S. N. Majumdar, A. Comtet, and J. Randon-Furling, Exact Distribution of the Maximal Height of p Vicious Walkers, *Phys. Rev. Lett.* **101**, 150601 (2008).
- [29] E. Brunet and B. Derrida, Statistics at the tip of a branching random walk and the delay of traveling waves, *Europhys. Lett.* **87**, 60010 (2009).
- [30] J. Rambeau and G. Schehr, Distribution of the time at which N vicious walkers reach their maximal height, *Phys. Rev. E* **83**, 061146 (2011).
- [31] E. S. Andersen, On the fluctuations of sums of random variables, *Math. Scand.* **2**, 195 (1954).
- [32] S. N. Majumdar, A. Rosso, and A. Zoia, Time at which the maximum of a random acceleration process is reached, *J. Phys. A: Math. Theor.* **43**, 115001 (2010).
- [33] T. W. Burkhardt, Semiflexible polymer in the half plane and statistics of the integral of a Brownian curve, *J. Phys. A: Math. Gen.* **26**, L1157 (1993).
- [34] P. Singh, Random acceleration process under stochastic resetting, *J. Phys. A: Math. Theor.* **53**, 405005 (2020).
- [35] P. Singh and A. Kundu, Generalised ‘Arcsine’ laws for run-and-tumble particle in one dimension, *J. Stat. Mech.* (2019) 083205.
- [36] F. Mori, P. Le Doussal, S. N. Majumdar and G. Schehr, Universal Survival Probability for a d -Dimensional Run-and-Tumble Particle, *Phys. Rev. Lett.* **124**, 090603 (2020).
- [37] K. J. Wiese, S. N. Majumdar, and A. Rosso, Perturbation theory for fractional Brownian motion in presence of absorbing boundaries, *Phys. Rev. E* **83**, 061141 (2011).
- [38] T. Sadhu, M. Delorme, and K. J. Wiese, Generalized Arcsine Laws for Fractional Brownian Motion, *Phys. Rev. Lett.* **120**, 040603 (2018).
- [39] S. N. Majumdar, A. Rosso, and A. Zoia, Hitting Probability for Anomalous Diffusion Processes, *Phys. Rev. Lett.* **104**, 020602 (2010).
- [40] G. Schehr and P. Le Doussal, Extreme value statistics from the real space renormalization group: Brownian motion, Bessel processes and continuous time random walks, *J. Stat. Mech.* (2010) P01009.
- [41] D. S. Dean and S. N. Majumdar, Large Deviations of Extreme Eigenvalues of Random Matrices, *Phys. Rev. Lett.* **97**, 160201 (2006).
- [42] S. N. Majumdar and M. Vergassola, Large Deviations of the Maximum Eigenvalue for Wishart and Gaussian Random Matrices, *Phys. Rev. Lett.* **102**, 060601 (2009).
- [43] S. N. Majumdar and G. Schehr, Top eigenvalue of a random matrix: Large deviations and third order phase transition, *J. Stat. Mech.* (2014) P01012.
- [44] S. Raychaudhuri, M. Cranston, C. Przybyla, and Y. Shapir, Maximal Height Scaling of Kinetically Growing Surfaces, *Phys. Rev. Lett.* **87**, 136101 (2001).
- [45] S. N. Majumdar and A. Comtet, Exact Maximal Height Distribution of Fluctuating Interfaces, *Phys. Rev. Lett.* **92**, 225501 (2004).
- [46] J. Rambeau and G. Schehr, Extremal statistics of curved growing interfaces in 1+1 dimensions, *Europhys. Lett.* **91**, 60006 (2010).
- [47] S. N. Majumdar, Real-space condensation in stochastic mass transport models, in *Exact Methods in Low-Dimensional Statistical Physics and Quantum Computing: Lecture Notes of the Les Houches Summer School*, July 2008, edited by J. Jacobsen, S. Ouvry, V. Pasquier, D. Serban, and L. Cugliandolo (Oxford University Press, Oxford, 2010), Vol. 89, p. 407.
- [48] A. Guillet, E. Roldán, and F. Jülicher, Extreme-value statistics of stochastic transport processes, *New J. Phys.* **22**, 123038 (2020).
- [49] M. R. Evans and S. N. Majumdar, Condensation and extreme value statistics, *J. Stat. Mech.* (2008) P05004.
- [50] S. N. Majumdar and J. P. Bouchaud, Optimal time to sell a stock in the Black-Scholes model: Comment on ‘Thou Shalt Buy and Hold’, by A. Shiryaev, Z. Xu, and X. Y. Zhou, *Quant. Finance* **8**, 753 (2008).
- [51] Y. V. Fyodorov and J. P. Bouchaud, Freezing and extreme-value statistics in a random energy model with logarithmically correlated potential, *J. Phys. A: Math. Theor.* **41**, 372001 (2008).
- [52] A. Bar, S. N. Majumdar, G. Schehr, and D. Mukamel, Exact extreme-value statistics at mixed-order transitions, *Phys. Rev. E* **93**, 052130 (2016).
- [53] M. Höll, W. Wang, and E. Barkai, Extreme value theory for constrained physical systems, *Phys. Rev. E* **102**, 042141 (2020).
- [54] L. Frachebourg, I. Ispolatov, and P. L. Krapivsky, Extremal properties of random systems, *Phys. Rev. E* **52**, 5727(R) (1995).
- [55] C. Godreche, S. N. Majumdar, and G. Schehr, Longest Excursion of Stochastic Processes in Nonequilibrium Systems, *Phys. Rev. Lett.* **102**, 240602 (2009).
- [56] M. R. Leadbetter, G. Lindgren, and H. Rootzén, *Extremes and Related Properties of Random Sequences and Processes* (Springer Science & Business Media, New York, 1983).
- [57] R. A. Fisher and L. H. C. Tippett, Limiting forms of the frequency distribution of the largest or smallest member of a sample, *Math. Proc. Cambridge Philos. Soc.* **24**, 180 (1928).
- [58] B. Gnedenko, Sur la distribution limite du terme maximum d’une série aléatoire, *Ann. Math.* **44**, 423 (1943).

- [59] E. J. Gumbel, *Statistics of Extremes* (Dover, New York, 1958).
- [60] J. Y. Fortin and M. Clusel, Applications of extreme value statistics in physics, *J. Phys. A: Math. Theor.* **48**, 183001 (2015).
- [61] S. Albeverio, V. Jentsch, and H. Kantz (eds.), *Extreme Events in Nature and Society* (Springer Science & Business Media, Berlin, 2006).
- [62] S. N. Majumdar, A. Pal, and G. Schehr, Extreme value statistics of correlated random variables: A pedagogical review, *Phys. Rep.* **840**, 1 (2020).
- [63] J. P. Bouchaud and M. Mézard, Universality classes for extreme-value statistics, *J. Phys. A: Math. Gen.* **30**, 7997 (1997).
- [64] S. Sabhapandit, Extremes and records, [arXiv:1907.00944](https://arxiv.org/abs/1907.00944).
- [65] S. N. Majumdar, Universal first-passage properties of discrete-time random walks and Lévy flights on a line: Statistics of the global maximum and records, *Physica A* **389**, 4299 (2010).
- [66] E. Dumonteil, S. N. Majumdar, A. Rosso, and A. Zoia, Spatial extent of an outbreak in animal epidemics, *Proc. Natl. Acad. Sci. USA* **110**, 4239 (2013).
- [67] S. N. Majumdar and P. L. Krapivsky, Extreme value statistics and traveling fronts: Application to computer science, *Phys. Rev. E* **65**, 036127 (2002).
- [68] S. N. Majumdar, Traveling front solutions to directed diffusion-limited aggregation, digital search trees, and the Lempel-Ziv data compression algorithm, *Phys. Rev. E* **68**, 026103 (2003).
- [69] P. L. Krapivsky and S. N. Majumdar, Traveling Waves, Front Selection, and Exact Nontrivial Exponents in a Random Fragmentation Problem, *Phys. Rev. Lett.* **85**, 5492 (2000).
- [70] J. Randon-Furling, S. N. Majumdar, and A. Comtet, Convex Hull of N Planar Brownian Motions: Exact Results and an Application to Ecology, *Phys. Rev. Lett.* **103**, 140602 (2009).
- [71] F. Mori, S. N. Majumdar, and G. Schehr, Time Between the Maximum and the Minimum of a Stochastic Process, *Phys. Rev. Lett.* **123**, 200201 (2019).
- [72] F. Mori, S. N. Majumdar, and G. Schehr, Distribution of the time between maximum and minimum of random walks, *Phys. Rev. E* **101**, 052111 (2020).
- [73] S. N. Majumdar, Brownian functionals in physics and computer science, *Curr. Sci.* **89**, 2076 (2005).
- [74] A. Dhar and S. N. Majumdar, Residence time distribution for a class of Gaussian Markov processes, *Phys. Rev. E* **59**, 6413 (1999).
- [75] S. N. Majumdar and D. S. Dean, Exact occupation time distribution in a non-Markovian sequence and its relation to spin glass models, *Phys. Rev. E* **66**, 041102 (2002).
- [76] S. N. Majumdar and A. Comtet, Local and the Occupation Time of a Particle Diffusing in a Random Medium, *Phys. Rev. Lett.* **89**, 060601 (2002).
- [77] S. Sabhapandit, S. N. Majumdar, and A. Comtet, Statistical properties of functionals of the paths of a particle diffusing in a one-dimensional random potential, *Phys. Rev. E* **73**, 051102 (2006).
- [78] F. den Hollander, S. N. Majumdar, J. M. Meylahn, and H. Touchette, Properties of additive functionals of Brownian motion with resetting, *J. Phys. A: Math. Theor.* **52**, 175001 (2019).
- [79] A. Comtet, F. Cornu, and G. Schehr, Last-passage time for linear diffusions and application to the emptying time of a box, *J. Stat. Phys.* **181**, 1565 (2020).
- [80] A. Comtet and J. Desbois, Brownian motion in wedges, last passage time and the second arc-sine law, *J. Phys. A* **36**, L255 (2003).
- [81] H. Boutcheng, T. Bouetou, T. W. Burkhardt, A. Rosso, A. Zoia, and K. T. Crepin, Occupation time statistics of the random acceleration model, *J. Stat. Mech.* (2016) 053213.
- [82] S. Carmi, L. Turgeman, and E. Barkai, On distributions of functionals of anomalous diffusion paths, *J. Stat. Phys.* **141**, 1071 (2010).
- [83] P. C. Bressloff, Occupation time of a run-and-tumble particle with resetting, *Phys. Rev. E* **102**, 042135 (2020).
- [84] D. Charles and W. Rosemarie, The arc sine law and the treasury bill futures market, *Financial Analysts J.* **36**, 71 (1980).
- [85] A. N. Shiryaev, Quickest detection problems in the technical analysis of the financial data, in *Mathematical Finance Bachelor Congress 2000* (Springer, New York, 2002), p. 487.
- [86] A. Baldassarri, J. P. Bouchaud, I. Dornic, and C. Godrèche, Statistics of persistent events: An exactly soluble model, *Phys. Rev. E* **59**, 20(R) (1999).
- [87] C. Godrèche and J. M. Luck, Statistics of the occupation time of renewal processes, *J. Stat. Phys.* **104**, 489 (2001).
- [88] S. Burov and E. Barkai, Residence Time Statistics for N Renewal Processes, *Phys. Rev. Lett.* **107**, 170601 (2011).
- [89] Y. Kasahara, Limit theorems of occupation times for Markov processes, *Publ. RIMS, Kyoto Univ.* **12**, 801 (1977).
- [90] J. Lamperti, An occupation time theorem for a class of stochastic processes, *Trans. Am. Math. Soc.* **88**, 380 (1958).
- [91] A. C. Barato, E. Roldán, I. A. Martínez, and S. Pigolotti, Arcsine Laws in Stochastic Thermodynamics, *Phys. Rev. Lett.* **121**, 090601 (2018).
- [92] R. Dey, A. Kundu, B. Das, and A. Banerjee, Experimental verification of arcsine laws in mesoscopic non-equilibrium and active systems, [arXiv:2104.00127](https://arxiv.org/abs/2104.00127).
- [93] G. Bel and E. Barkai, Weak Ergodicity Breaking in the Continuous-Time Random Walk, *Phys. Rev. Lett.* **94**, 240602 (2005).
- [94] E. Barkai, Residence time statistics for normal and fractional diffusion in a force field, *J. Stat. Phys.* **123**, 883 (2006).
- [95] N. G. van Kampen, Itô versus Stratonovich, *J. Stat. Phys.* **24**, 175 (1981).
- [96] A. W. C. Lau and T. C. Lubensky, State-dependent diffusion: Thermodynamic consistency and its path integral formulation, *Phys. Rev. E* **76**, 011123 (2007).
- [97] M. Kac, On distributions of certain Wiener functionals, *Trans. Am. Math. Soc.* **65**, 1 (1949).
- [98] S. Redner, *A Guide to First-Passage Processes* (Cambridge University Press, Cambridge, 2001).
- [99] See Supplemental Material at <http://link.aps.org/supplemental/10.1103/PhysRevE.105.024113> for more details on the computations.
- [100] W. Feller, *An Introduction to Probability Theory and Its Applications* (Wiley, New York, 1968).
- [101] A. G. Cherstvy, W. Wang, R. Metzler, and I. M. Sokolov, Inertia triggers nonergodicity of fractional Brownian motion, *Phys. Rev. E* **104**, 024115 (2021).